PRIFYSGOL
BANGOR
UNIVERSITY

Drought-related mortality modifies mixing effects on light absorption and growth in mono-specific and mixed stands of Fagus sylvatica, Alnus glutinosa and Betula pendula.

Plaga, Benjamin; Bauhus, Jürgen; Smith, Andy; Gonzalez Pereira, Mario ; Forrester, David

Forestry

Drought-related mortality modifies mixing effects on light absorption and growth in mono-specific and mixed stands of Fagus sylvatica, Alnus glutinosa and Betula pendula

Benjamin N. E. Plaga[1], Jürgen Bauhus[1], Andrew R. Smith[2], Mário Gonzalez Pereira[3], David I. Forrester[4*]

[1]Chair of Silviculture, Institute of Forest Sciences, Faculty of Environment and Natural Resources, University of Freiburg, Tennenbacherstrasse 4, 79106 Freiburg, Germany

[2]Environment Centre Wales, School of Natural Sciences, Bangor University, Bangor, Gwynedd, LL57 2DG, UK

[3]Centre for Research and Technology of Agro-Environmental and Biological Sciences (CITAB), Inov4Agro, University of Trás-os-Montes and Alto Douro (UTAD), Quinta de Prados, 5000-801 Vila Real, Portugal

[4]CSIRO Environment, GPO Box 1700, Canberra, ACT 2601, Australia

*Corresponding author: Email: David.Forrester@csiro.au

Little is known about how drought-related mortality influences light absorption of surviving trees and consequent changes in tree species interactions. Here, we used the detailed tree-level light model (Maestra) in combination with measurements of tree dimensions, crown architectures and stand structures to examine experimental mixing effects of *Fagus sylvatica*, *Alnus glutinosa* and *Betula pendula* on light dynamics following a drought in Bangor, Wales. The experimental stands, planted in 2004, were composed of clusters with 1 – 3 species in different combinations. Droughts occurred in 2011 and 2014 during the growing seasons, and trees were measured in 2014 and 2015. Species mixing resulted, on average, in higher tree growth, absorption of photosynthetically active radiation (APAR) and light use efficiency (LUE) compared to the mean of the monocultures. An exception was the monoculture of *Betula pendula* which was the most productive species, and had higher growth, APAR or LUE than some mixtures. Drought-related mortality reduced stand basal area across all plots by an average of 8.3% and tree density by 11%. This moderate change in structure did not result in significant increases in individual tree APAR, LUE, or growth. From a management perspective, mortality might need to reduce stand density more strongly than it did in this study before light absorption or light-use efficiency are altered.

Introduction

The increasing frequency, duration, and intensity of droughts is impacting different types of forest ecosystems in many regions of the world (IPCC, 2013). Tree mortality rates are increasing in many forest types and climate zones as a consequence of, drought, water stress, and the subsequently increased activity of biotic agents (Allen *et al.*, 2010, 2015). This mortality can strongly modify stand structure and thus ecosystem functioning (Klos *et al.*, 2009; Lindner *et al.*, 2010; Anderegg *et al.*, 2013; Bennett *et al.*, 2015; Clark *et al.*, 2016; Seidl *et al.*, 2017). To assess potential options to increase the resilience and adaptive capacity of forests in relation to climate change, it is important to know how mortality-driven changes in structure influence ecosystem functions and services. Processes such as light absorption, light-use efficiency, and subsequent growth of remaining trees will likely play a central role in the ecosystem response to tree mortality.

Currently, establishing mixed-species forests is seen as one of the main strategies to increase resistance, resilience, and adaptive capacity in relation to climatic change (Bauhus *et al.*, 2017a; Messier *et al.*, 2022), in addition, mixed species forests can be more productive than the mean of the individual species monocultures (Zhang *et al.*, 2012; Jactel *et al.*, 2017; Feng *et al.*, 2022). One of the causes of the higher productivity of mixtures is light-related species interactions (Binkley *et al.*, 1992; Forrester *et al.*, 2012, 2018; Sapijanskas *et al.*, 2014). Absorption of photosynthetically active radiation (APAR) and light use efficiency (LUE) in mixtures are influenced by canopy stratification (Binkley *et al.*, 1992; Forrester *et al.*, 2012; le Maire *et al.*, 2013), different crown shapes and architectures (Bauhus *et al.*, 2004; Sapijanskas *et al.*, 2014; Forrester *et al.*, 2018), interspecific differences in physiology and phenology (Binkley *et al.*, 1992; Augspurger and Bartlett, 2003; Lopez *et al.*, 2008; Forrester *et al.*, 2012; Vitasse, 2013; Sapijanskas *et al.*, 2014; Gressler *et al.*, 2015), and stand density (Will *et al.*, 2005; Forrester et al., 2013, 2018; Sapijanskas *et al.*, 2014; Dong *et al.*, 2016).

Increases in canopy tree mortality rates may alter the interactions between species within mixtures. Mortality leads to open spaces in forest canopies, similar to thinning from above, and can also change the vertical structure by removing species or trees that occupy specific positions within the canopy, e.g. a thinning from below that removes overtopped and intermediate trees or subcanopy species. Thinning usually leads to an increase in the productivity of the residual trees (Smith *et al.*, 1997; Bauhus *et al.*, 2017b) which may partly be caused by an increase in APAR or LUE of retained individual trees. West and Osler (1995) found an increase in individual tree growth after thinning on two sites of *Eucalyptus regnans*, which resulted from higher individual tree APAR. When there was no understory, thinning also resulted in higher individual tree LUE. Increases in individual tree APAR and LUE following thinning have also been reported in other studies (Forrester *et al.*, 2013; Gspaltl *et al.*, 2013). Tree loss by mortality, although a more gradual process than tree removal through thinning, could have similar effects to thinning on APAR, LUE and growth.

Unlike thinning, the effect of natural mortality on APAR and LUE in mixed-species forests has received very little attention. Therefore, the objective of this study was to examine how mortality in a tree diversity experiment influenced tree and stand APAR and LUE. The experiment contained plots with 1, 2 and 3 species-mixtures of *Fagus sylvatica, Alnus glutinosa* and *Betula pendula* in Bangor,

78 Wales. All plots that were examined for this study included drought-induced tree mortality and were
79 measured in the year that followed the drought.

80 We tested the following hypotheses:

81 1) Increases in APAR and LUE are both responsible for complementary effects on tree growth in
82 mixtures compared with monocultures.

83 2) Intra-specific differences in crown architecture (in addition to inter-specific differences) contribute
84 to increases in APAR and LUE in mixtures.

85 3) A reduction in stand density due to mortality results in an increase in individual tree growth, APAR
86 and LUE.

87

88 **Methods**
89 *Site description & Experimental design*
90 The investigations took place in some of the plots within the BangorDIVERSE experiment which is
91 part of TreeDivNet, a global network of tree diversity experiments. It was established with a total
92 area of 2.36 ha in March 2004 at the Henfaes Research Centre of Bangor University in Wales (UK)
93 (53° 14' 16.382''N, 4° 1' 0.922''W) at 13 – 18 m a.s.l near the coast (Ahmed *et al.*, 2016). Soils
94 are classified as Eutric Fluvic Cambisols (IUSS Working Group WRB., 2006) (Fluventic Dystrochrept,
95 USDA system) and have fine loamy texture (Smith *et al.*, 2013).
96 The experiment has a hexagonal planting design where each species was planted with an inter-tree
97 spacing of 1×1 m (10 000 trees ha^{-1}). Each hexagonal plot originally contained 94 trees and a two-
98 row buffer strip with an additional 78 trees. In the plots that were examined in this study the species
99 pool containing *Alnus glutinosa*, *Betula pendula* and *Fagus sylvatica* was used to create a diversity
100 gradient comprising one-, two-, and three-species communities. This study was performed inll
101 species combinations (n=7) that occurred in oval or circular clusters of trees (Figure 1) and each of
102 the hexagonal plots was replicated five times, totalling 35 clusters. The two-row buffer strip
103 combined with the gradual change in species composition within each hexagon, from one cluster to
104 the next, is expected to minimise any potential edge effects between species combinations. During
105 data collection late in the summer of 2015, it was noticed that a considerable proportion of trees
106 had died since the inventory in 2014. Using the meteorologically data that were logged on-site, we
107 found that since the beginning of the experiment, we identified droughts occurring in 2011 and
108 2014, especially during the growing seasons when only half of the long-term average precipitation
109 occurred (Table 1). Prior to 2011 there had been negligible mortality within the plots.

110

111 *Quantification of the vertical structure and distribution of leaf area and leaf-area density*
112 All tree diameters at 1.3 m (DBH) were measured in April 2014 and September 2015. To quantify the
113 leaf area and leaf-area density distribution of each tree, we took detailed tree measurements for each
114 of the three species on one individual in each species combination (cluster) and replicated it in each

115   plot in 2015. This procedure included measuring the following variables: diameter at 1.30 m, height,
116   live-crown length, crown area, as well as the diameters, heights, and cardinal directions (divided into 8
117   segments: N, NE, E, SE, S, SW, W, NW) of all branches on each of the sample trees. In addition, the
118   mean branch angle from the horizontal was estimated for each quarter of the live-crown length. A
119   sample branch was then taken from each quarter of these target trees to measure the mean leaf
120   angles from the horizontal, the branch length, leaf area, and leaf dry mass. For the latter, all leaves
121   were removed from the sample branches, dried at 70°C, and weighed. Before drying, the leaf area of
122   a subsample was determined using the leaf area meter LI-3050C Transparent Belt Conveyor Accessory
123   (LI-COR Biosciences GmbH, Bad Homburg, Germany) to calculate the specific leaf area (m^2 kg^{-1}) for the
124   branch and thus the leaf area from the product of specific leaf area and leaf-dry weight of the branch.
125   In the next step, we used the branch measurements to develop allometric equations (as shown in
126   Equation 1) for each species to calculate all branch lengths within the crowns and the leaf area of all
127   target trees.

$$\ln(Y) = \ln\beta_0 + \beta_1 \ln(d_b) + \beta_2 \ln(rh) + \beta_3 (\ln(d_b) * \ln(rh)) + \varepsilon \qquad (1)$$

128

129   Where Y is branch length or branch leaf area, d_b is branch diameter, rh is relative height of the branch
130   within the live-crown length (base = 1, top = 0), and ε is a correction ratio used when back-
131   transforming the ln- transformed Y- variables. The correction ratio was calculated as the sum of the
132   measured values divided by the sum of the (back-transformed) predicted values (Snowdon, 1991). All
133   allometry parameters are shown in the supporting information. The leaf area of a given branch was
134   assumed to be distributed evenly between the base of the branch, where it joined the tree stem,
135   and the height of the branch tips, which was calculated using the branch length and branch angle
136   measurements as described in Medhurst and Beadle (2001) and Forrester *et al.* (2013). In the last
137   step, the leaf area density (LAD, m^2 m^{-3}) was calculated by dividing the total crown into 10 layers. Each
138   layer contributed 10% of the live-crown length, and was assumed to have a volume of a semi-elliptical
139   cone for the top layer or a frustum of a semi-elliptical cone for the other nine layers (Equation 2). The
140   vertical distribution of LAD was fitted to a beta distribution (Equation 3, Wang et al., 1990) where the
141   LAD of a layer was a function of its relative height within the crown. The parameters of this
142   equation are required inputs to run the Maestra model (Grace *et al.*, 1987; Wang and Jarvis, 1990;
143   Medlyn, 2004; Duurma and Medlyn, 2012), which was used to calculate individual tree APAR.

144

$$V = \frac{2}{3}\pi * h * r^2 + \sum_{l=2}^{10} h * (d_{basal}^2 + d_{top}^2 + d_{basal} * d_{top}) * \frac{\pi}{12} \qquad (2)$$

145

146   Where V is the total crown volume, h the height of the layer, r is the radius of the cone for the top
147   layer, d_{basal} is the crown diameter of the base of the frustrum and d_{top} the crown diameter of the top.

148

$$Y = a(x^b) * (1-x)^{cc} \qquad (3)$$

149   Where a, b and cc are fitted parameters, and Y is the leaf area density (m^2 m^{-3}) at a relative height
150   of x within the canopy.

151

Field measurements and quantification of structure and growth at the tree and stand levels

152 *Field measurements and quantification of structure and growth at the tree and stand levels*
153 In addition to the target trees mentioned above for which we measured individual tree leaf area (*la*),
154 crown diameter and vertical distribution of LAD, we also measured height and live-crown length for
155 all trees within the plot, as well as DBH of all trees within the plot and the surrounding buffer trees. For
156 all other trees, including buffer trees, the height, leaf area, crown diameter, and live crown
157 length were determined by predicting these variables as a function of DBH, separately for each
158 species (Equation 4).

$$\ln (Y) = \ln\beta_0 + \beta_1 \ln (DBH) + \varepsilon \tag{4}$$

159 Where *Y* is height, leaf area, crown diameter, and live crown length, and ε is a correction ratio used
160 when back-transforming the ln- transformed *Y*- variables. The correction ratio was calculated as the
161 sum of the measured values divided by the sum of the (back-transformed) predicted values (Snowdon,
162 1991). Individual crown volumes (m³) were calculated for each tree from their crown diameter
163 and live-crown length by assuming semi-elliptical shapes (Equation 2).
164 Individual tree basal area increment (cm² year^{-1}) was calculated by combining the DBH measurements
165 from 2015 with those of the previous inventory in 2014. We also recorded trees that had recently died
166 due to drought. This allowed us to use our allometric equations to calculate all variables for trees
167 that were alive in the previous inventory. We were therefore able to quantify the structure of the plots
168 before and after the drought-related tree death. The Maestra model was then used to calculate the
169 individual tree APAR for two cases: a) following the mortality event (all trees that have died have no
170 leaves) and b) for the same structure as if no trees had died during the drought, assuming all trees still
171 have leaves.
172 Stand variables calculated included the relative height, mean stand height (m), tree density (trees ha^{-1}
173 $^{-1}$), leaf area index (m² m^{-2}) basal area (m² ha^{-1}), basal area increment (m² ha^{-1} year^{-1}), canopy depth (m),
174 canopy-volume(m³ ha^{-1}) and canopy–leaf area density (m² m^{-3}). The relative height of a given species
175 was calculated as the mean height of the target species divided by the mean height of the
176 total cluster. The canopy depth was calculated from the difference between the hight of
177 the tallestestspan style="font-family:Calibri"> tree in a cluster and the height of the crown base of
178 the tree with the lowest crown in that cluster.
179 To illustrate the change in stand structure caused by drought-related mortality, we examined
180 diameter distributions corrected for the species proportions (Supplementary Figures S1-S3; Figure 3).
181 That is, the number of trees in each diameter class was divided by the proportion of stand basal
182 area contributed by that species (not by the diameter class). The trend curves (Figure 3) were
183 obtained using Friedman's SuperSmoother (Friedman, 1984b, 1984a) to smooth the (x,y) values. We
184 used the R function 'supsmu', from the 'stats' package and R 4.0.3 (R Core Team, 2020), which is a
185 running lines smoother which chooses between three spans for the lines (Friedman, 1984b, 1984a).
186 The running lines smoothers are symmetric, with k/2 data points on each side of the predicted point,
187 and values of k as 0.5 × n, 0.2 × n and 0.05 × n, where n is the number of data points. The best of the
188 three smoothers was chosen by cross-validation for each prediction. The best spans were then
189 smoothed using the running lines smoother and the final prediction chosen by linear interpolation.
190
191 *Climate data*

192 We obtained meteorological data from the ERA-Interim reanalysis daily dataset produced by the
193 European Centre for Medium-Range Weather Forecasts (ECMWF) with a high spatial
194 resolution (0.125° × 0.125°) (Dee *et al.*, 2011). The climatic variables included monthly and daily mean
195 temperature, precipitation, solar radiation and thnumber of frost days. We extracted daily data
196 on surface solar radiation downwards (SSRD), from 2012 to 2017 and monthly climate data from 1979
197 to 2017. In addition, we obtained on-site meteorological data (based on hourly means) from
198 the Henfaes Research Centre of Bangor University for 2004 – 2014 to determine the precipitation
199 pattern for this period. The solar radiation was used as input to the Maestra model to calculate APAR
200 and LUE.
201

202 *MAESTRA Light modelling to estimate APAR*
203 Individual tree APAR was calculated using the MAESTRA model (Grace *et al.*, 1987; Wang and Jarvis,
204 1990; Medlyn, 2004; Duursma and Medlyn, 2012). This 3D tree-level model calculates individual
205 trees' APAR based on their individual crown architecture (e.g. crown dimensions and leaf area and leaf
206 angle distributions), leaf optical properties (LAD and distribution, leaf transmittance and reflectance),
207 and the shading from neighbouring trees based on the positions of other trees within the plot (defined
208 by x and y coordinates, the slope and aspect of the site) and their crown architectures (e.g. Figure 2).
209 The growing season has been defined by the site-specific phenology of the leaf-bearing period of the
210 three species we studied. This was from Julian day 111 to Julian day 303. APAR was calculated for the
211 growing season (defined by the leaf-bearing period) and also for the whole year. The parameterization
212 data we used are provided in Supplementary Table S1.
213

214 *Estimation of LUE and relative productivity (RP)*
215 Tree level LUE (cm^2 GJ^{-1}) was calculated as the basal area increment of the individual tree (cm^2 $year^{-1}$)
216 per APAR (GJ $year^{-1}$). Stand level LUE (m^2 GJ^{-1}) was calculated as the basal area increment of the whole
217 community (cluster) (m^2 ha^{-1} $year^{-1}$) per APAR (GJ ha^{-1} $year^{-1}$).
218 The relative productivity variable (Equations 5 and 6) quantifies whether mixing led to an increase
219 (RP>1) or decrease (RP<1) in a given variable compared to a monoculture at the stand level, per
220 species (Equation), or the whole plot community (Equation 5) (Williams and McCarthy, 2001;
221 Forrester and Pretzsch, 2015). The RP also accounts for the proportion of the species in the mixtures,
222 which was quantified in terms of leaf area index (LAI; m^2 m^{-2}) or stand basal area, depending on the
223 response variable. For response variables tree density, basal area and basal area increment, we
224 quantified the species proportions in terms of stand basal area. All other proportions for the canopy
225 and light variables (canopy-depth, -volume, -proportion of canopy filled with tree crowns, -LAD, APAR
226 and LUE) were quantified in terms of LAI because it is considered more representative of the species
227 contributions to light dynamics, and species proportions by leaf area have been shown to provide
228 realistic estimates of species proportions on an area basis (Dirnberger and Sterba, 2014).

$$\mathrm{RP_{community}} = \frac{p_{mix^{sp1, sp2, ...}}}{::_{sp1}p_{mono^{sp1}} + ::_{sp2}p_{mono^{sp2}} + ...} \tag{5}$$

229

$$\mathrm{RP_{species}} = \frac{p_{mix^{sp1,(sp2...)}}}{::_{sp1}p_{mono^{sp1}}}$$
(6)

230 In Equation 5,   is the productivity (or the performance of another response variable) of the
231 mixed species stand in relation to the productivity of their related monocultures (,   )
232 and their proportional (,   ) amount on LAI or stand basal area depending on the stand variable
233 considered. Equation 6 is used to determine the relative productivity by species where   is
234 the productivity of a given species (sp1) in a mixture with (sp2).

235

236 *Statistical analysis*
237 Differences between species mixing treatments or between species were examined using a Tukey test.
238 All variables were visually assessed for normality. Regression models were fitted as hierarchical mixed-
239 effects models using the R package nlme (Pinheiro *et al.*, 2020) and R 4.0.3 (R Core Team, 2020). To
240 ensure that residuals were centred at zero and approximately normally distributed, the residual and
241 normal quantile plots were assessed. For branch-level regressions, the random effect was tree nested
242 within plot, and for tree-level regressions the random effect was the plot.

243

244 **Results**
245 *Tree level effects of mixing, mortality, and stand structure*
246 Across all clusters, the highest mortality rate occurred in *A. glutinosa* which resulted in a 21%
247 reduction in basal area and a 32% reduction in tree density (Supplementary Table S2). The greatest
248 reduction in *A. glutinosa* density occurred in the 3-species mixture and included trees from all
249 diameter classes. In the monoculture and 2-species mixtures, mortality decreased from smaller to
250 medium diameter classes (Supplementary Figure S2 (a-d)).
251 For *A. glutinosa*, DBH, height, live-crown length, and crown volume were larger in the mixture
252 with *B. pendula* than in monoculture (Table 2). When in combination
253 with *F. sylvatica*, *B. pendula* crown parameters were not significantly larger, but DBH and leaf
254 area were higher compared to monocultures (Table 2). We found these differences in terms
255 of the mixture before as well as after tree mortality, but we found no effect within the mixtures and
256 within the monoculture due to mortality. When *A. glutinosa* and *B. pendula* were mixed with the
257 smaller *F. sylvatica*, the relative height increased accordingly for both species and decreased
258 for *F. sylvatica*. APAR was higher for the trees in 2-species mixtures without any *B. pendula* compared
259 to the trees in monocultures or the 3-species mixture. This mixing effect only occurred for stands
260 containing *B. pendula* after the occurrence of mortality (Table 2) which, was the largest in
261 these clusters. Basal area growth and light use efficiency increased when growing
262 with *F. sylvatica* (Table 2).
263 Drought-related mortality decreased the basal area of *B. pendula* by 3.1% and tree density by 9.9%
264 (Supplementary Table S2). Only the smallest diameter classes were affected and almost all of
265 them were in the monoculture and the 3-species mixture (Supplementary Figure S3 (a-d)). Nearly all
266 examined tree variables, except LUE, increased for *B. pendula* when mixed with *F. sylvatica* (Table 2).
267 In contrast, when *B. pendula* was combined with *A. glutinosa* or was in the 3-species mixture, there

268 were no significant changes in its tree-level variables when compared to the monoculture. There was
269 no significant effect on these mixing results due to mortality within these clusters.
270 Unlike *B. pendula*, *F. sylvatica* showed a reduction in some variables in the 2-species combination
271 with *B. pendula* (Table 2). Since basal area growth remained the same, while a reduction in APAR
272 occurred, this led to a higher LUE compared to monocultures (Table 2). The relative height
273 of *F. sylvatica* was reduced by the presence of the two taller tree species in mixtures. Nevertheless,
274 with *A. glutinosa* as a neighbour, *F. sylvatica* was able to increase live-crown length, leaf area, crown
275 volume and also APAR (Table 2). In the 3-species mixture, in addition to the higher live-crown length,
276 crown volume, and APAR, *F. sylvatica* even achieved higher basal area growth as well as an increase
277 in LUE (Table 2). Mortality in *F. sylvatica* was negligible.
278 We did not detect any major shifts in species proportions due to mortality (Figure 3 e-l). However,
279 there were small shifts in tree size distributions towards larger diameter classes
280 for *B. pendula* and *A. glutinosa* , while for *F. sylvatica*, the smallest species, the mortality of the other
281 two species caused a corresponding shift towards the smaller diameter classes (Figure 3 e-l).
282 Individual tree APAR was positively correlated with tree leaf area for all species
283 (Supplementary Figure S4). For a given tree leaf area, APAR of *B. pendula* was significantly greater in
284 3-species mixtures and when combined with *F. sylvatica*, but significantly lower when mixed
285 with *A. glutinosa* than in monocultures. *A. glutinosa* in a mixture with *F. sylvatica* and in 3-species
286 mixture had a significantly greater APAR for a given leaf area compared to their monoculture.
287 For *F. sylvatica* APAR remained the same as in all treatments (Supplementary Figure S4).
288
289 *Stand level effects of mixing and mortality*
290 Mortality within clusters reduced basal area by 8.3% and density by 11% (Supplementary Table S2).
291 As the smaller and medium diameter classes within the two larger species were mainly affected by
292 mortality, there was a decrease in the frequency of these diameters for the total stands of the 2- and
293 3-species mixtures (Figure 3 a-d). The visual inspection ofhe diameter class distribution was only
294 changed by mortality in the 3-species mixture, where we observed a shift toward the smaller diameter
295 classes (Figure 3 d).
296 The two-species mixture of *F. sylvatica* and *B. pendula* showed higher tree density, LAI, canopy depth,
297 canopy volume *,* and a higher proportion of filled canopy space when compared to the monoculture
298 of *B. pendula* (Supplementary Table S3,   Figure 4 a, c).   Compared   to
299 the *F. sylvatica* monoculture canopy depth and canopy volume as well as basal area and basal area
300 growth were also higher in the mixture (Supplementary Table S3; Figure 4 a, d). Both species absorbed
301 more   PAR   in   2-species   mixture   than   the   respective   monocultures
302 (Figure 4 e; Supplementary Table S3). The mixture of these species also achieved the highest overall
303 values in terms of canopy volume, LAI, basal area increment and APAR compared to all other clusters
304 (Figure 4 a, c-e).
305 The combination of *B. pendula* and *A. glutinosa* led to higher total means of LAI, canopy depth,
306 canopy voume, basal area, and basal area increment as well as higher APAR when compared with the
307 monoculture   of A. *glutinosa* but   not   when   compared   with   the *B. pendula* monoculture
308 (Supplementary Table S3; Figure 4 a, c-e).

309 The 2-species mixture of *F. sylvatica* and *A. glutinosa* resulted in higher tree density, LAI, canopy

310 depth, canopy voume, proportion of filled canopy space, and APAR in comparison to the monoculture

311 of *A. glutinosa,* and higher canopy depth, and basal area , but lower proportion of filled canopy space,

312 than in the *F. sylvatica* monoculture (Supplementary Table S3, Figure 4 a, c, e). Both basal area

313 increment and LUE were also higher in the mixture than in respective monocultures. Here, after the

314 onset of mortality LUE for *A. glutinosa* became higher in the mixture than in the monoculture

315 (Supplementary Table S3; Figure 4 f). No other mortality effects were significant.

316 The 3-species mixture showed higher tree density, LAI, canopy depth, canopy volume, proportion of

317 canopy space filled, and APAR when compared with *A. glutinosa* monocultures and lower tree

318 density and proportion of canopy space filled, but higher basal area and canopy depth, when

319 compared with *F.&#a0;sylvatica* monocultures before and after the drought-related mortality, except

320 APAR which was also higher in the 3-species mixture before mortality than

321 in *F. sylvatica* monocultures (Supplementary Table S3; Figure 4 b, c, e). There were no significant

322 differences between response variables in *B. pendula* between its monoculture and the 3-species

323 mixture, except for *canopy depth.* This pattern did not change with the following mortality.

324

325 *Diversity level effects of mixing and mortality*

326 On average, mortality reduced basal area across the three diversity levels by 16.2% across all 3-species

327 mixtures, 8.9% across all monocultures and 5.2% in the 2-species mixtures (Supplementary Table S2).

328 In terms of diversity level, 2-species mixtures benefited most compared to monocultures regarding

329 nearly all variables (Supplementary Table S4, Figure 5 a, c-f). The 3-species mixtures also

330 benefited compared to monocultures, except for tree density, basal area and LUE

331 (Supplementary Table S4; Figure 5 a, c-e). The canopy leaf area density was highest in monocultures

332 and significantly lower in the mixtures, which then did not differ further among the different mixtures.

333 Within a diversity level, mortality only led to a significant reduction in tree density in the 3-species

334 mixture (Supplementary Table S4). As a result of this mortality, the APAR of 3-species mixtures was

335 significantly lower than in 2-species mixtures, which was not the case before the mortality

336 occurred (Figure 5 e). In contrast, mortality within the 3-species mixtures resulted in a slightly non-

337 significant increased LUE, which was then not statistically different from the 2-species

338 mixtures whereas this was the case before the mortality occurred. (Supplementary Table S4;

339 Figure 5 f).

340

341 **Discussion**

342

343 The basal area growth was lower, on average, in the monocultures (0.95 m^2 ha^{-1} yr^{-1}) than in the 2-

344 species mixtures (2.1 m^2 ha^{-1} yr^{-1}) and 3-species mixture (1.4 m^2 ha^{-1} yr^{-1}). This was associated with

345 higher APAR in the 2-species mixtures (18.3 GJ ha^{-1} 10^{-3}) and 3-species mixture (15.2 GJ ha^{-1} 10^{-3}) when

346 compared to the monocultures (11.3 GJ ha^{-1} 10^{-3}). The stand LUE was also higher in the 2-species

347 mixtures (109 m^2 GJ^{-1} $\times$ 10^6) and 3-species mixture (92 m^2 GJ^{-1} $\times$ 10^6) than in the monocultures

348 (73 m^2 GJ^{-1} $\times$ 10^6). These findings are in accordance with hypothesis 1 and with results from other

349 studies which showed that higher growth in mixtures is often associated with increases in both APAR

350 and LUE (Binkley *et al.*, 1992; Forrester *et al.*, 2012; Forrester and Albrecht, 2014; Forrester, 2019).
351 Here, this result is predominantly attributable to tree species identity effects. For example *B.*
352 *pendula* was generally more productive and had higher APAR and LUE than the other species and
353 also maintained these advantages when growing in mixtures (Figure 4 D-F). Similarly, LAI was highest
354 in *F. sylvatica* monocultures and when this species was present in the mixtures, it increased LAI and
355 canopy volumes in these stands. As a result, the *F. sylvatica-B. pendula* mixture had the highest APAR
356 of any treatment, regardless of mortality effects (Figure 4 a, c, e). Species identity appear to have been
357 an important determinant of mixing effects on growth and APAR in most studies (e.g., le Maire *et al.*,
358 2013; Forrester *et al.*, 2019). This enhancement of APAR, and hence the growth of mixtures, was
359 probably at least partly caused by inter-specific differences in tree size (crowns, heights, crown
360 lengths), crown architecture (leaf angles), tree allometry and the effect these had on canopy attributes
361 (e.g. varying leaf area density, canopy stratification, canopy volume). Inter-specific differences in
362 physiology, such as photosynthetic rates, LUE and the often observed synergistic effect of mixing fast-
363 growing shade-intolerant species with initially slow-growing shade-tolerant species, may also have
364 contributed to mixing effects on LUE, as was found in previous studies (Binkley *et al.*, 1992;
365 Forrester *et al.*, 2012; Baeten *et al.*, 2019; Serrano-León *et al.*, 2022).
366 Differences in growth or light absorption have also been linked to intra-specific differences in
367 physiology, mean tree sizes, crown architectures (e.g. leaf angles), and allometric relationships
368 between stem size and crown characteristics (Sapijanskas *et al.*, 2014; Dong *et al.*, 2016; Forrester *et*
369 *al.*, 2018; Serrano-León *et al.*, 2022). In this study, there were only minor differences in allometric
370 relationships (e.g. Figure S4) and specific leaf area for a given species in the different species
371 combinations. Therefore, intra-specific variability may not have been as important in these stands.
372 There were also negligible shifts in the partitioning of light between size classes, such that competition
373 for light for all species was generally size-symmetric or slightly asymmetric as indicated by the linear
374 relationships between individual tree leaf area and APAR (Figure S4). While these findings contradict
375 our second hypothesis that intra-specific differences in crown architecture (in addition to inter-
376 specific differences) contribute to increases in APAR and LUE in these mixtures, similar results have
377 been obtained in previous studies (e.g. Forrester, 2019; Plaga et al., "in review").
378 The drought-related mortality reduced stand basal area by only 8.5% and tree density by 11%. This
379 minor reduction in stand density had no significant influence on stand growth, APAR or LUE and no
380 influence on individual tree growth following the drought. This is consistent with many thinning
381 studies showing that minor changes in stand density (< 20% reduction in basal area) have little
382 influence on growth (Stoneman *et al.*, 1996; Mäkinen and Isomäki, 2004; Will *et al.*, 2005). Studies
383 that found such effects on growth and APAR were typically conducted at much higher thinning
384 intensities, for example with a 65% reduction in tree density (Forrester, 2013) or a 74% reduction in
385 basal area (West and Osler, 1995; Gspaltl *et al.*, 2013). This indicates that unless mortality removes
386 much larger proportions of stand density, it is unlikely to influence APAR.
387 Given the strong correlation between radiation, temperature and vapour pressure deficit under forest
388 canopies, the minimal effects of mortality on APAR in this study may be associated with minimal
389 effects on below canopy microclimates. Therefore, mortality or thinning events that remove small
390 proportions of overstorey stand basal area may have a negligible influence on the ability of forests to

391 function as an insulator for understorey communities (Davis et al. 2013; von Arx et al.
392 2012; Zellweger et al. 2020).

393 A small effect of mortality could only be observed for *A. glutinosa*, where mortality reduced their basal
394 area across all stands by 21% and even 63% in the 3-species stands (Supplementary Table S2) in which
395 all diameter classes of *A. glutinosa* were affected. This supports our assessment that APAR or LUE
396 will only change significantly when larger proportions of the stand density die . The reason for the
397 much higher drought-related mortality in *A. glutinosa* may be attributed to its preference for moist to
398 wet soil conditions (Houston Durrant *et al.*, 2016; CABI, 2022). Although we observed a few small
399 changes in growth, APAR and LUE due to mortality, the gradient in mortality across the experiment
400 was too small to robustly test the third hypothesis, that a reduction in stand density due to mortality
401 results in an increase in individual tree growth, APAR and LUE. Changes in the structure after
402 drought could probably similarly influence APAR, but for this to happen, the effects of drought must
403 be much stronger than in this study.

404

405 The results of this study should be interpreted with caution when extrapolating to other forests given
406 the young age of this experiment (10 years old), the high planting density of 10,000 plants per ha, and
407 the strong influence that site conditions (e.g. resource availability and climatic conditions) can have
408 on mixing effects. Crowns may be more responsive at this age than in older stands, and as trees age
409 there are changes in crown architecture and morphology (e.g. specific leaf area, leaf angle
410 distributions), and canopy structure that can influence APAR. Furthermore, drought can influence
411 mortality for several years following the end of a drought and our data collected only one year after
412 the drought may hence not yet capture all effects induced by the drought (Bigler *et al.*, 2006, 2007;
413 Cailleret *et al.*, 2017; Klockow *et al.*, 2018; Powers *et al.*, 2020; Trugman *et al.*, 2021).
414 In our experiment, there was negligible mortality prior to 2011, and therefore, we assume that the
415 majority of mortality in this study was caused by drought. Trees that appeared to be dying in 2015 did
416 not recover, and we assumed there was negligible additional mortality after our measurements until
417 another severe drought in 2018, so it is likely that the major influence of the 201and 2015 drought on
418 APAR was quantified. Given that all plots were influenced by the drought, it is not possible to
419 distinguish the effect of changes in density on tree growth and LUE from those caused by water stress
420 during the drought.

421 The magnitudes of the mixing effects found in this study should not be extrapolated to other sites
422 given that the relative sizes of mixing effects on growth can change with resource availability and
423 climatic conditions (e.g. Forrester, 2014). These spatial dynamics of mixing effects could be examined
424 by replicating mixtures along site gradients in resource availability and climatic conditions. They could
425 also be predicted using process-based models that have been validated for their ability to predict
426 mixing effects in forests, such as the 3-PG model (e.g. Forrester et al., 2017a).

427 The estimates of APAR obtained using the Maestra model in this study will be influenced by
428 the model inputs for each individual tree. It was not possible to measure the leaf areas, vertical crown
429 leaf area density distributions, or leaf angles for all trees and therefore allometric relationships were
430 used. Allometric relationships between tree size and foliage mass or area for a given species can when
431 it is growing in a mixture with other species (e.g. Laclau et al., 2008) and stand density
432 (e.g. Monserud and Marshall, 1999; Forrester et al., 2017b). Similarly, mixing can influence the

433   vertical distribution of leaf area within tree crowns (Garber and Maguire, 2005; Binkley, 1992).
434   Therefore trees from all treatments were sampled and used to derive the inputs for the Maestra
435   model. We assume that the APAR estimates used in this study are reliable because the mixing effects
436   on allometry and vertical crown leaf area density distributions were accounted for, and several studies
437   have found accurate comparisions between Maestra predictions of APAR and observed APAR or APAR
438   estimated using hemispherical photography (Charbonnier et al. 2013; le Maire et al. 2013; Forrester
439   et al. 2018, 2019).

Conclusion

In conclusion, species mixing increased growth, APAR and LUE compared with the mean of the monocultures, with the exception of the most productive monoculture of *B. pendula*. The reduction in stand density caused by drought-related mortality was too small to notably influence APAR, LUE or growth. This is consistent with previous studies where greater reductions in density by thinning were required to significantly increase APR. With regards to forest management, minor reductions in stand density may be unlikely to cause significant effects on stand APAR, LUE, or growth.

Conflict of interest statement
None declared

Data availability statement
The data underlying this article will be shared on reasonable request to the corresponding author.

References

472   Ahmed, I.U., Smith, A.R., Jones, D.L., and Godbold, D.L. 2016 Tree species identity
473   influences the vertical distribution of labile and recalcitrant carbon in a temperate
474   deciduous forest soil, For. Ecol. Manage., 359, 352–360. doi: 10.1016/j.foreco.2015.07.018.

475   Allen, C.D., Macalady, A.K., Chenchouni, H., Bachelet, D., McDowell, N., Vennetier, M., et al.
476   2010 A global overview of drought and heat-induced tree mortality reveals emerging
477   climate change risks for forests, For. Ecol. Manage., 259(4), 660–684. doi:
478   10.1016/j.foreco.2009.09.001.

479   Allen, C.D., Breshears, D.D., and McDowell, N.G. 2015 On underestimation of global
480   vulnerability to tree mortality and forest die-off from hotter drought in the Anthropocene,
481   Ecosphere, 6(8), 1–55. doi: 10.1890/ES15-00203.1.

482   Anderegg, W.R.L., Kane, J.M., and Anderegg, L.D.L. 2013 Consequences of widespread tree
483   mortality triggered by drought and temperature stress, Nat. Clim. Chang., 3(1), 30–36. doi:
484   10.1038/nclimate1635.

485   Augspurger, C.K., and Bartlett, E.A. 2003 Differences in leaf phenology between juvenile and
486   adult trees in a temperate deciduous forest, Tree Physiol., 23(8), 517–525. doi:
487   10.1093/treephys/23.8.517.

488   Baeten, L., Bruelheide, H., van der Plas, F., Kambach, S., Ratcliffe, S., Jucker, T., et al. 2019
489   Identifying the tree species compositions that maximize ecosystem functioning in European
490   forests, J. Appl. Ecol., 56(3), 733–744. doi: 10.1111/1365-2664.13308.

491   Bauhus, J., Forrester, D.I., Gardiner, B., Jactel, H., Vallejo, R., and Pretzsch, H. 2017a
492   Ecological stability of mixed-species forests, in H. Pretzsch, D.I. Forrester, and J. Bauhus (eds)
493   Mix. For. - Ecol. Manag. Springer, Berlin, Heidelberg, 337–382. doi: 10.1007/978-3-662-
494   54553-9_7.

495   Bauhus, J., Forrester, D.I., Pretzsch, H., Felton, A., Pyttel, P., and Benneter, A. 2017b
496   Silvicultural options for mixed-species stands, in H. Pretzsch, D.I. Forrester, and J. Bauhus
497   (eds) Mix. For. Ecol. Manag. Springer Berlin Heidelberg, 433–501. doi: 10.1007/978-3-662-
498   54553-9_9.

499   Bauhus, J., Van Winden, A.P., and Nicotra, A.B. 2004 Aboveground interactions and
500   productivity in mixed-species plantations of Acacia mearnsii and Eucalyptus globulus, Can. J.
501   For. Res., 34(3), 686–694. doi: 10.1139/x03-243.

502   Bennett, A.C., McDowell, N.G., Allen, C.D., and Anderson-Teixeira, K.J. 2015 Larger trees
503   suffer most during drought in forests worldwide, Nat. Plants, 1(10), 15139. doi:
504   10.1038/nplants.2015.139.

505   Bigler, C., Bräker, O.U., Bugmann, H., Dobbertin, M., and Rigling, A. 2006 Drought as an
506   Inciting Mortality Factor in Scots Pine Stands of the Valais, Switzerland, Ecosystems, (9),
507   330–343. doi: 10.1007/s10021-005-0126-2.

508   Bigler, C., Gavin, D.G., Gunning, C., and Veblen, T.T. 2007 Drought induces lagged tree
509   mortality in a subalpine forest in the Rocky Mountains, Oikos, 116(July), 1983–1994. doi:
510   10.1111/j.2007.0030-1299.16034.x.

511 Binkley, D., 1992. Mixtures of nitrogen-fixing and non-nitrogen-fixing tree species. In:
512 Cannell, M.G.R., Malcolm, D.C., Robertson, P.A. (Eds.), The ecology of mixed species stands
513 of trees. Blackwell Scientific, London, pp. 99-123.

514 Binkley, D., Dunkin, K.A., DeBell, D., and Ryan, M.G. 1992 Production and Nutrient Cycling in
515 Mixed Plantations of Eucalyptus and Albizia in Hawaii, For. Sci., 38(2), 393–408. doi:
516 10.1093/forestscience/38.2.393.

517 CABI 2022 Alnus glutinosa (European alder), CABI Compend. CABI International. doi:
518 10.1079/cabicompendium.4574.

519 Cailleret, M., Jansen, S., Robert, E.M.R., Desoto, L., Aakala, T., Antos, J.A., et al. 2017 A
520 synthesis of radial growth patterns preceding tree mortality, Glob. Chang. Biol., (23), 1675–
521 1690. doi: 10.1111/gcb.13535.

522 Charbonnier, F., Maire, G.l., Dreyer, E., Casanoves, F., Christina, M., Dauzat, J., Eitel, J.U.H.,
523 Vaast, P., Vierling, L.A., Roupsard, O., 2013. Competition for light in heterogeneous
524 canopies: Application of MAESTRA to a coffee (Coffea arabica L.) agroforestry system.
525 Agricultural and Forest Meteorology 181, 152-169.

526 Clark, J.S., Iverson, L., Woodall, C.W., Allen, C.D., Bell, D.M., Bragg, D.C., et al. 2016 The
527 impacts of increasing drought on forest dynamics, structure, and biodiversity in the United
528 States, Glob. Chang. Biol., 22(7), 2329–2352. doi: 10.1111/gcb.13160.

529 Davis, K.T., Dobrowski, S.Z., Holden, Z.A., Higuera, P.E., Abatzoglou, J.T., 2018. Microclimatic
530 buffering in forests of the future: the role of local water balance. Ecography 41, 1-11.

531 Dee, D.P., Uppala, S.M., Simmons, A.J., Berrisford, P., Poli, P., Kobayashi, S., et al. 2011 The
532 ERA-Interim reanalysis: Configuration and performance of the data assimilation system, Q. J.
533 R. Meteorol. Soc., 137(656), 553–597. doi: 10.1002/qj.828.

534 Dirnberger, G.F., and Sterba, H. 2014 A comparison of different methods to estimate species
535 proportions by area in mixed stands, For. Syst., 23(3), 534–546. doi: 10.5424/fs/2014233-
536 06027.

537 Dong, T.L., Forrester, D.I., Beadle, C., Doyle, R., Hoang, N.H., Giap, N.X., et al. 2016 Effects of
538 light availability on crown structure, biomass production, light absorption and light-use
539 efficiency of Hopea odorataplanted within gaps in Acacia hybrid plantations, Plant Ecol.
540 Divers., 9(5–6), 535–548. doi: 10.1080/17550874.2016.1262471.

541 Duursma, R.A., and Medlyn, B.E. 2012 MAESPA: A model to study interactions between
542 water limitation, environmental drivers and vegetation function at tree and stand levels,
543 with an example application to [CO2] × drought interactions, Geosci. Model Dev., 5(4), 919–
544 940. doi: 10.5194/gmd-5-919-2012.

545 Feng, Y., Schmid, B., Loreau, M., Forrester, D.I., Fei, S., Zhu, Jianxiao, et al. 2022 Multispecies
546 forest plantations outyield monocultures across a broad range of conditions, Science (80-.).
547 doi: 10.1126/science.abm6363.

548 Forrester, D.I., 2014. The spatial and temporal dynamics of species interactions in mixed-
549 species forests: From pattern to process. Forest Ecology and Management 312, 282-292.

Forrester, D.I., Lancaster, K., Collopy, J.J., Warren, C.R., and Tausz, M. 2012 Photosynthetic capacity of Eucalyptus globulus is higher when grown in mixture with Acacia mearnsii, Trees - Struct. Funct., 26(4), 1203–1213. doi: 10.1007/s00468-012-0696-5.

Forrester, D.I., Collopy, J.J., Beadle, C.L., and Baker, T.G. 2013 Effect of thinning, pruning and nitrogen fertiliser application on light interception and light-use efficiency in a young Eucalyptus nitens plantation, For. Ecol. Manage., 288, 21–30. doi: 10.1016/j.foreco.2011.11.024.

Forrester, D.I. 2013 Growth responses to thinning, pruning and fertiliser application in Eucalyptus plantations: A review of their production ecology and interactions, For. Ecol. Manage., 310, 336–347. doi: 10.1016/j.foreco.2013.08.047.

Forrester, D.I., Ammer, C., Annighöfer, P.J., Barbeito, I., Bielak, K., Bravo-Oviedo, A., et al. 2018 Effects of crown architecture and stand structure on light absorption in mixed and monospecific Fagus sylvatica and Pinus sylvestris forests along a productivity and climate gradient through Europe, J. Ecol., 106(2), 746–760. doi: 10.1111/1365-2745.12803.

Forrester, D.I., Ammer, C., Annighöfer, P.J., Avdagic, A., Barbeito, I., Bielak, K., Brazaitis, G., Coll, L., Río, M.d., Drössler, L., Heym, M., Hurt, V., Löf, M., Matović, B., Meloni, F., Ouden, J.d., Pach, M., Pereira, M.G., Ponette, Q., Pretzsch, H., Skrzyszewski, J., Stojanović, D., Svoboda, M., Ruiz-Peinado, R., Vacchiano, G., Verheyen, K., Zlatanov, T., Bravo-Oviedo, A., 2017a. Predicting the spatial and temporal dynamics of species interactions in Fagus sylvatica and Pinus sylvestris forests across Europe Forest Ecology and Management 405, 112-133.

Forrester, D.I., Tachauer, I.H.H., Annighoefer, P., Barbeito, I., Pretzsch, H., Ruiz-Peinado, R., Stark, H., Vacchiano, G., Zlatanov, T., Chakraborty, T., Saha, S., Sileshi, G.W., 2017b. Generalized biomass and leaf area allometric equations for European tree species incorporating stand structure, tree age and climate. Forest Ecology and Management 396, 160-175.

Forrester, D.I. 2019 Linking forest growth with stand structure: Tree size inequality, tree growth or resource partitioning and the asymmetry of competition, For. Ecol. Manage., 447(March), 139–157. doi: 10.1016/j.foreco.2019.05.053.

Forrester, D.I., Rodenfels, P., Haase, J., Härdtle, W., Leppert, K.N., Niklaus, P.A., et al. 2019 Tree-species interactions increase light absorption and growth in Chinese subtropical mixed-species plantations, Oecologia, 191(2), 421–432. doi: 10.1007/s00442-019-04495-w.

Forrester, D.I., and Albrecht, A.T. 2014 Light absorption and light-use efficiency in mixtures of Abies alba and Picea abies along a productivity gradient, For. Ecol. Manage., 328, 94–102. doi: 10.1016/j.foreco.2014.05.026.

Forrester, D.I., and Pretzsch, H. 2015 Tamm Review: On the strength of evidence when comparing ecosystem functions of mixtures with monocultures, For. Ecol. Manage., 356, 41–53. doi: 10.1016/j.foreco.2015.08.016.

Friedman J.H. 1984a A variable span scatterplot smoother. Laboratory for Computational Statistics, Stanford University Technical Report No.5.

590 Friedman J.H. 1984b User's Guide. Laboratory for Computational Statistics, Stanford
591 University Technical Report No1. Available at: https://purl.stanford.edu/pd898dq6156.

592 Garber, S.M., Maguire, D.A., 2005. The response of vertical foliage distribution to spacing
593 and species composition in mixed conifer stands in central Oregon. Forest Ecology and
594 Management 211, 341-355.

595 Grace, J.C., Jarvis, P.G., and Norman, J.M. 1987 Modelling the interception of solar radiant
596 energy in intensively managed stands, New Zeal. J. For. Sci., 17(2–3), 193–209.

597 Gressler, E., Jochner, S., Capdevielle-Vargas, R.M., Morellato, L.P.C., and Menzel, A. 2015
598 Vertical variation in autumn leaf phenology of Fagus sylvatica L. in southern Germany, Agric.
599 For. Meteorol., 201, 176–186. doi: 10.1016/j.agrformet.2014.10.013.

600 Gspaltl, M., Bauerle, W., Binkley, D., and Sterba, H. 2013 Leaf area and light use efficiency
601 patterns of Norway spruce under different thinning regimes and age classes, For. Ecol.
602 Manage., 288, 49–59. doi: 10.1016/j.foreco.2011.11.044.

603 Houston Durrant, T., de Rigo, D., and Caudullo, G. 2016 Alnus glutinosa in Europe:
604 distribution, habitat, usage and threats, Eur. Atlas For. Tree Species, 64–65.

605 IPCC 2013 The Physical Science Basis. Contribution of Working Group I to the Fifth
606 Assessment Report of the Intergovern- mental Panel on Climate Change. Edited by T.F.
607 Stocker et al. Cambridge University Press, Cambridge, United Kingdom and New York, NY,
608 USA. doi: 10.1017/CBO9781107415324.Summary.

609 IUSS Working Group WRB. 2006 World reference base for soil resources 2006. 2nd edn.
610 Rome: World Soil Resources Reports No. 103. FAO. Available at:
611 ftp://ftp.fao.org/agl/agll/docs/wsrr103e.pdf.

612 Jactel, H., Bauhus, J., Boberg, J., Bonal, D., Castagneyrol, B., Gardiner, B., et al. 2017 Tree
613 Diversity Drives Forest Stand Resistance to Natural Disturbances, Curr. For. Reports, 3(3),
614 223–243. doi: 10.1007/s40725-017-0064-1.

615 Klockow, P.A., Vogel, J.G., Edgar, C.B., and Moore, G.W. 2018 Lagged mortality among tree
616 species four years after an exceptional drought in east Texas, Ecosphere, 9(10)(October).
617 doi: 10.1002/ecs2.2455.

618 Klos, R.J., Wang, G.G., Bauerle, W.L., and Rieck, J.R. 2009 Drought impact on forest growth
619 and mortality in the southeast USA: An analysis using Forest Health and Monitoring data,
620 Ecol. Appl., 19(3), 699–708. doi: 10.1890/08-0330.1.

621 Laclau, J.-P., Bouillet, J.-P., Gonçalves, J.L.M., Silva, E.V., Jourdan, C., Cunha, M.C.S., Moreira,
622 M.R., Saint-André, L., Maquère, V., Nouvellon, Y., Ranger, J., 2008. Mixed-species
623 plantations of Acacia mangium and Eucalyptus grandis in Brazil 1. Growth dynamics and
624 aboveground net primary production. Forest Ecology And Management 255, 3905-3917.

625 Lindner, M., Maroschek, M., Netherer, S., Kremer, A., Barbati, A., Garcia-Gonzalo, J., et al.
626 2010 Climate change impacts, adaptive capacity, and vulnerability of European forest
627 ecosystems, For. Ecol. Manage., 259(4), 698–709. doi: 10.1016/j.foreco.2009.09.023.

628 Lopez, O.R., Farris-Lopez, K., Montgomery, R.A., and Givnish, T.J. 2008 Leaf phenology in
629 relation to canopy closure in southern Appalachian trees, Am. J. Bot., 95(11), 1395–1407.
630 doi: 10.3732/ajb.0800104.

631 le Maire, G., Nouvellon, Y., Christina, M., Ponzoni, F.J., Gonçalves, J.L.M., Bouillet, J.P., et al.
632 2013 Tree and stand light use efficiencies over a full rotation of single- and mixed-species
633 Eucalyptus grandis and Acacia mangium plantations, For. Ecol. Manage., 288, 31–42. doi:
634 10.1016/j.foreco.2012.03.005.

635 Mäkinen, H., and Isomäki, A. 2004 Thinning intensity and growth of Scots pine stands in
636 Finland, For. Ecol. Manage., 201, 311–325. doi: 10.1016/j.foreco.2004.07.016.

637 Martonne, E. de. 1926 Une Nouvelle Fonction Climatologique: L'Indice d'Aridite (A New
638 Climatological Function: The Aridity Index), in La Météorolgie 2. Paris, 449–458.

639 Medhurst, J.L., and Beadle, C.L. 2001 Crown structure and leaf area index development in
640 thinned and unthinned </i>Eucalyptus nitens</i> plantations, Tree Physiol., 21(12–13), 989–
641 999. doi: 10.1093/treephys/21.12-13.989.

642 Medlyn, B. 2004 A MAESTRO retrospective., in M. Mencuccini et al. (eds) For. Land-
643 atmosph. interface. Sydney: CAB International 2004, 105–121. doi:
644 10.1079/9780851996776.0105.

645 Messier, C., Bauhus, J., Sousa-silva, R., Auge, H., Baeten, L., Barsoum, N., et al. 2022 For the
646 sake of resilience and multifunctionality , let ' s diversify planted forests !, Conserv. Lett.,
647 (July 2021), 1–8. doi: 10.1111/conl.12829.

648 Monserud, R.A., Marshall, J.D., 1999. Allometric crown relations in three northern Idaho
649 conifer species. Canadian Journal of Forest Research 29, 521-535.

650 Piepho, H.-P. 2004 An algorithm for a letter-based representation of all pairwise
651 comparisons, J. Comput. Graph. Stat., 13(2), 456–466.

652 Pinheiro, J., Bates, D., DebRoy, S., Sarkar, D., and (2020), R.C.T. 2020 _nlme: Linear and
653 Nonlinear Mixed Effects Models_. Available at: https://cran.r-project.org/package=nlme.

654 Plaga, B.N.E., Bauhus, J., Pretzsch, H., Pereira, M.G., and Forrester, D.I. no date Influence of
655 crown architecture and canopy structure on light absorption, light-use efficiency and growth
656 in mixed and pure Pseudotsuga menziesii and Fagus sylvatica forests, Eur. J. For. Res.
657 [Preprint]. doi: 'in review'.

658 Powers, J.S., Vargas G., G., Brodribb, T.J., Schwartz, N.B., Pérez-aviles, D., Smith-Martin,
659 C.M., et al. 2020 A catastrophic tropical drought kills hydraulically vulnerable tree species,
660 Glob. Chang. Biol., (26), 3122–3133. doi: 10.1111/gcb.15037.

661 R Core Team 2020 R: A Language and Environment for Statistical Computing. Vienna,
662 Austria: R Foundation for Statistical Computing. Available at: https://www.r-project.org/.

663 Sapijanskas, J., Paquette, A., Potvin, C., Kunert, N., and Loreau, M. 2014 Tropical tree
664 diversity enhances light capture through crown plasticity and spatial and temporal niche
665 differences, Ecology, 95(9), 2479–2492. doi: 10.1890/13-1366.1.

666   Seidl, R., Thom, D., Kautz, M., Martin-Benito, D., Peltoniemi, M., Vacchiano, G., et al.
667   2017 Forest disturbances under climate change, Nat. Clim. Chang., 7(6), 395–402. doi:
668   10.1038/nclimate3303.

669   Serrano-León, H., Nitschke, R., Scherer-Lorenzen, M., and Forrester, D.I. 2022 Intra-specific
670   leaf trait variability of F. sylvatica, Q. petraea and P. abies in response to inter-specific
671   competition and implications for forest functioning, Tree Physiol., 42(2), 253–272. doi:
672   10.1093/treephys/tpab109.

673   Smith, A.R., Lukac, M., Hood, R., Healey, J.R., Miglietta, F., and Godbold, D.L. 2013 Elevated
674   CO_2 enrichment induces a differential biomass response in a mixed species temperate
675   forest plantation, New Phytol., 198(1), 156–168. doi: 10.1111/nph.12136.

676   Smith, D.M., Larson, B.C., Kelty, M.J., and Ashton, M.S. (eds) 1997 The Practice of
677   Silviculture: Applied Forest Ecology. 9th edn. New York: Wiley.

678   Snowdon, P. 1991 A ration estimator for bias correction in logarithmic regressions, Can. J.
679   For. Res., 21(5), 720–724. doi: 10.1139/x91-101.

680   Stoneman, G.L., Crombie, D.S., Whitford, K., Hingston, F.J., Giles, R., Portlock, C.C., et al.
681   1996 Growth and water relations of Eucalyptus marginata (jarrah) stands in response to
682   thinning and fertilization, Tree Physiol., 16, 267–274.

683   Trugman, A.T., Anderegg, L.D.., Anderegg, W.R.., Das, A.J., and Stephenson, N.L. 2021 Why is
684   Tree Drought Mortality so Hard to Predict?, Trends Ecol. Evol., 36(6), 520–532. doi:
685   10.1016/j.tree.2021.02.001.

686   Vitasse, Y. 2013 Ontogenic changes rather than difference in temperature cause understory
687   trees to leaf out earlier, New Phytol., 198(1), 149–155. doi: 10.1111/nph.12130.

688   von Arx, G., Dobbertin, M., Rebetez, M., 2012. Spatio-temporal effects of forest canopy on
689   understory microclimate in a long-term experiment in Switzerland. Agricultural and Forest
690   Meteorology 166-167, 144-155.

691   Wang, Y.P., and Jarvis, P.G. 1990 Description and validation of an array model - MAESTRO,
692   Agric. For. Meteorol., 51(3–4), 257–280. doi: 10.1016/0168-1923(90)90112-J.

693   Wang, Y.P., Jarvis, P.G., and Benson, M.L. 1990 Two-dimensional needle-area density
694   distribution within the crowns of Pinus radiata, For. Ecol. Manage., 32(2–4), 217–237. doi:
695   10.1016/0378-1127(90)90172-8.

696   West, P.W., and Osler, G.H.R. 1995 Growth response to thinning and its relation to site
697   resources in Eucalyptus regnans, Can. J. For. Res., 25(1), 69–80. doi: 10.1139/x95-009.

698   Will, R.E., Narahari, N. V., Shiver, B.D., and Teskey, R.O. 2005 Effects of planting density on
699   canopy dynamics and stem growth for intensively managed loblolly pine stands, For. Ecol.
700   Manage., 205(1–3), 29–41. doi: 10.1016/j.foreco.2004.10.002.

701   Williams, A.C., and McCarthy, B.C. 2001 A new index of interspecific competition for
702   replacement and additive designs, Ecol. Res., 16(1), 29–40.

703   Zellweger, F., Frenne, P.D., Lenoir, J., Vangansbeke, P., Verheyen, K., Bernhardt-
704   Römermann, M., Baeten, L., Hédl, R., Berki, I., Brunet, J., Calster, H.V., Chudomelová, M.,
705   Decocq, G., Dirnböck, T., Durak, T., Heinken, T., Jaroszewicz, B., Kopecký, M., Máliš, F.,
706   Macek, M., Malicki, M., Naaf, T., Nagel, T.A., Ortmann-Ajkai, A., Petrík, P., Pielech, R.,
707   Reczynska, K., Schmidt, W., Standovár, T., Swierkosz, K., Teleki, B., Vild, O., Wulf, M.,
708   Coomes, D., 2020. Forest microclimate dynamics drive plant responses to warming. Science
709   368, 772-775.

710   Zhang, Y., Chen, H.Y.H., and Reich, P.B. 2012 Forest productivity increases with evenness,
711   species richness and trait variation: A global meta-analysis, J. Ecol., 100(3), 742–749. doi:
712   10.1111/j.1365-2745.2011.01944.x.

713   **Table and Figure captions**

714   **Figure 1**. Planting design of the mixing experiment hexagonal plots, which was replicated five times;
715   A_x with green dot = *A. glutinosa*; B_x with blue dot = *B. pendula*; F_x with red dot = *F. sylvatica*; $Ex_{x,x}$ with
716   black dots = buffer trees. The ovals with solid borderlines indicate mono-specific clusters, the
717   ovals with dashed lines indicate clusters with two-species mixtures, and circles with dashed
718   lines comprise tree clusters with the three-species mixture. The design minimises edge effects by
719   placing similar cluster next to each other. Edge effects were not addressed in the analysis.

720   **Figure 2:** 3-D representation of one plot with all seven clusters without the buffer tree rows illustrating
721   the canopy structure in terms of vertical stratification, canopy gaps and closure, horizontal
722   overlapping and interlocking of the crowns. Trees with green crowns represent *F. sylvatica*, grey
723   represents *B. pendula* and golden brown shows *A. glutinosa*.

724   **Figure 3** Size distributions illustrating the change in stand structure caused by drought-related
725   mortality in *A. glutinosa – B. pendula* stands (a,e,i), *A. glutinosa-F. sylvatica* stands (b,f,j), *B. pendula-
726   F. sylvatica* stands (c,g,k), and all 3 species (d,h,l). The size class is 1 cm. Trend curves were plotted by
727   the use of Friedman's SuperSmoother (Friedman J.H., 1984b, 1984a) to smooth the (x,y) values. Note
728   the different scales on the y-axes.

729   **Figure 4** Means of canopy volume (a), canopy leaf area density (b), leaf area index (c), stand basal area
730   increment (d), annual absorption of photosynthetic active radiation APAR (e), and light use efficiency
731   (f) with and without recently died trees across all monocultures and mixtures. *F. syl* = *F. sylvatica*, *B.
732   pen*= *B. pendula*, *A. glu* = *Alnus glutinosa* in monoculture. *B. pen F. syl*, *A. glu F. syl* and *A. glu F. syl* =
733   species combination in two species mixture. *A. glu, B. pen, F. syl* = three species mixture. Error bars
734   indicate the 95% confidence interval of LS mean. Means sharing a letter are not significantly different
735   (Tukey adjusted comparisons (p-value) with significance level alpha = 0.05; variables and
736   residuals were visually inspected for normality)
737

738   **Figure 5.** Means of canopy volume (a), canopy leaf area density (b), leaf area index (c), stand basal
739   area increment (d), annual absorption of photosynthetic active radiation APAR (e), and light use
740   efficiency (f) with and without recently died trees across all three diversity level. Error bars indicate
741   the 95% confidence interval of LS mean. Means sharing a letter are not significantly different (Tukey
742   adjusted comparisons (p-value) with significance level alpha = 0.05; variables and residuals were
743   visually inspected for normality)

744
745
746
747
748

749 **Table 1:** Mean annual precipitation, temperature and aridity index at the experiment. DOY are the
750 Julian days 111 and 303 of the year that define the growing season. The aridity index is calculated from
751 the amount of precipitation (P) and temperature (T) as P/(T+10) (Martonne, 1926).

	All year			Growing season - (DOY=111-303)		
	1979-2017	2011	2014	1979-2017	2011	2014
Precipitation (mm)	1013.1	471.8	621.2	567.4	270.8	270.4
Mean temperature (°C)	9.4	11.4	11.9	12.65	14.0	14.5
Aridity Index	52.2	22.1	28.4	25.1	11.5	11.1

752

753

Variable	Monoculture		2 species Mixture		2 species Mixture		3 species Mixture				p-value
F. sylvatica (n=145 | n=146)			+ *A. glutinosa*		+ *B. pendula*		+ *A. glutinosa* + *B. pendula*		div.level	mortality	interaction
Diameter (cm)	2.35 a	2.38 a	**2.75** a	**2.75** a	**1.93** b	**1.93** b	**2.56** a	**2.56** a	**<0.0001**	0.921	0.998
Height (m)	**4.17** a	**4.21** a	**4.59** a	**4.59** a	**3.58** b	**3.58** b	**4.25** a	**4.25** a	**<0.0001**	0.927	0.999
Crown diameter (m)	4.23 bc	4.26 ab	**4.57** a	**4.57** a	**3.93** c	**3.93** c	**4.37** ab	**4.37** ab	**<0.0001**	0.941	1
Live-crown length (m)	**2.89** a	**2.91** a	**3.70** b	**3.70** b	**2.61** a	**2.61** a	**3.49** b	**3.49** b	**<0.0001**	0.956	1
Height to the live crown (m)	**1.28** a	**1.3** a	**0.89** bc	**0.89** bc	**0.97** b	**0.97** b	**0.76** c	**0.76** c	**<0.0001**	0.926	0.999
Leaf area (m²) **	4.80 a	4.94 a	**6.87** b	**6.87** b	**3.33** c	**3.33** c	**5.81** ab	**5.81** ab	**<0.0001**	0.922	0.999
Crown volume (m³) **	**29.12** ac	**29.67** a	**43.87** b	**43.87** b	**22.33** c	**22.33** c	**36.93** b	**36.93** b	**<0.0001**	0.946	1
Relative height	**1** a	**1** a	**0.81** b	**0.83** b	**0.56** c	**0.56** c	**0.67** d	**0.68** d	**<0.0001**	0.671	0.972
APAR (GJ tree⁻¹ season⁻¹) *	0.79 a	0.84 ab	**1.21** bc	**1.31** c	**0.53** d	**0.56** ad	**1.16** bc	**1.25** c	**<0.0001**	0.487	1
APAR (MJ per tree per day)*	2.16 a	2.29 ab	**3.30** bc	**3.59** c	**1.45** d	**1.54** ad	**3.19** bc	**3.42** c	**<0.0001**	0.487	1
Basal area growth (cm² year⁻¹) *	**0.64** a	**0.65** a	0.74 ab	0.74 ab	**0.63** a	**0.63** a	**0.82** b	**0.82** b	**<0.0001**	0.946	1
Light use efficiency (cm² GJ⁻¹) *	**0.69** a	**0.69** a	**0.73** abd	**0.71** ab	**0.84** cd	0.82 bcd	**0.92** c	**0.89** c	**<0.0001**	0.513	0.974
B. pendula (n=132 | n=145)			+ *A. glutinosa*		+ *F. sylvatica*		+ *A. glutinosa* + *F. sylvatica*		div.level	mortality	interaction
Diameter (cm)	**5.46** a	**5.89** a	5.91 a	**5.91** a	**7.31** b	7.74 b	**5.87** a	**6.03** a	**0.0003**	0.427	0.960
Height (m)	7.83 b	8.25 ab	7.87 b	7.87 b	8.89 ab	9.23 a	8.09 b	8.25 ab	**0.019**	0.399	0.952

			+ B. pendula		+ F. sylvatica		+ B. pendula + F. sylvatica		div.level	mortality	interaction
Crown diameter (m) *	3.36 a	3.44 a	3.54 ac	3.54 ac	3.91 bc	4.03 b	3.54 a	3.58 ac	0.0006	0.461	0.972
Live crown length (m)	4.07 a	4.31 ab	4.48 ab	4.48 ab	5.15 bc	5.40 c	4.49 ab	4.59 ab	0.0045	0.488	0.976
Height to the live crown (m)	3.75 a	3.92 a	3.38 a	3.38 a	3.73 a	3.48 a	3.62 a	3.67 a	0.159	0.563	0.978
Leaf area (m²) **	4.58 a	5.14 a	5.28 ac	5.28 ac	7.16 bc	7.85 b	5.23 a	5.48 ac	0.0006	0.421	0.960
Crown volume (m³) *	29.31 a	33.05 ab	34.75 ab	34.75 ab	49.31 bc	56.15 c	34.75 ab	36.53 ab	0.002	0.454	0.967
Relative height	1 a	1 a	0.98 a	0.97 a	1.4 bc	1.44 b	1.27 c	1.32 bc	<0.0001	0.493	0.937
APAR (GJ per tree per season) *	1.95 a	2.47 a	2.15 a	2.26 a	4.16 bc	4.98 b	2.5 a	2.93 ac	0.0001	0.181	0.965
APAR (MJ per tree per day)*	5.34 a	6.72 a	5.90 a	6.14 a	11.41 bc	13.66 b	6.79 a	8.04 ac	0.0001	0.181	0.965
Basal area growth (cm² year^{-1}) *	2.53 a	2.77 ab	3.1 abc	3.1 abc	4.02 bc	4.57 c	2.72 ab	2.92 ab	0.009	0.489	0.982
Light use efficiency (cm² GJ^{-1})	0.90 a	0.83 a	0.97 a	0.93 a	0.84 a	0.92 a	0.74 a	0.73 a	0.219	0.883	0.943

A. glutinosa (n=42 | n=68)			+ B. pendula		+ F. sylvatica		+ B. pendula + F. sylvatica		div.level	mortality	interaction
Diameter (cm)	5.21 b	5.55 ab	6.41 ae	6.86 de	7.72 cd	8.46 c	6.05 abe	6.80 acde	<0.0001	0.091	0.947
Height (m)	6.94 b	7.23 ab	8.31 cd	8.89 c	7.99 acd	8.19 acd	7.48 abd	8.23 abcd	0.0005	0.133	0.902
Crown diameter (m)	3.12 b	3.22 ab	3.28 ab	3.38 ab	3.54 a	3.69 a	3.31 ab	3.51 ab	0.066	0.322	0.993
Live crown length (m)	3.19 a	3.18 a	4.38 bc	4.69 b	3.56 ac	3.60 abc	3.60 ac	3.72 abc	0.001	0.727	0.9770
Height to the live crown (m)	3.81 a	4.09 a	3.91 a	4.18 a	4.44 a	4.58 a	3.89 a	4.47 a	0.438	0.276	0.967
Leaf area (m²)	2.97 b	3.16 ab	4 abc	4.37 ac	4.32 c	4.73 c	3.7 abc	4.26 abc	0.002	0.272	0.979
Crown volume (m³) *	17.15 a	17.68 ab	27.44 bc	30.64 c	24.1 abc	25.33 abc	23.62 abc	26.9 abc	0.009	0.569	0.999
Relative height	1 a	1 a	1.06 ac	1.09 ac	1.36 b	1.43 b	1.9 cd	1.32 bd	<0.0001	0.179	0.689
APAR (GJ per tree per season)	1.15 a	1.41 ab	1.93 bc	2.40 c	2.42 c	2.76 c	1.89 bc	2.14 abc	<0.0001	0.134	0.986
APAR (MJ per tree per day)	3.15 a	3.87 ab	5.30 bc	6.57 c	6.61 c	7.55 c	5.17 bc	5.86 abc	<0.0001	0.134	0.986
Basal area growth (cm² year^{-1}) *	1.17 bc	1.23 abc	1.48 ab	1.82 ae	2.32 de	3.0 d	0.92 c	1.05 abc	<0.0001	0.187	0.884

Light use efficiency (cm² GJ⁻¹) **	0.58 ª	0.58ª	0.69 ᵃᶜ	0.95 ᵃᵇᶜ	1.95 ᵇᶜ	2.67ᵇ	0.15ª	0.24 ª	0.0001	0.492	0.933

761 APAR was predicted using the MAESTRA model.

762 * Values were ln-transformed before back transformed by Snowden-ratio (Snowdon, 1991).

763 ** Values were sqrt-transformed before back transformed by Snowden-ratio (Snowdon, 1991).
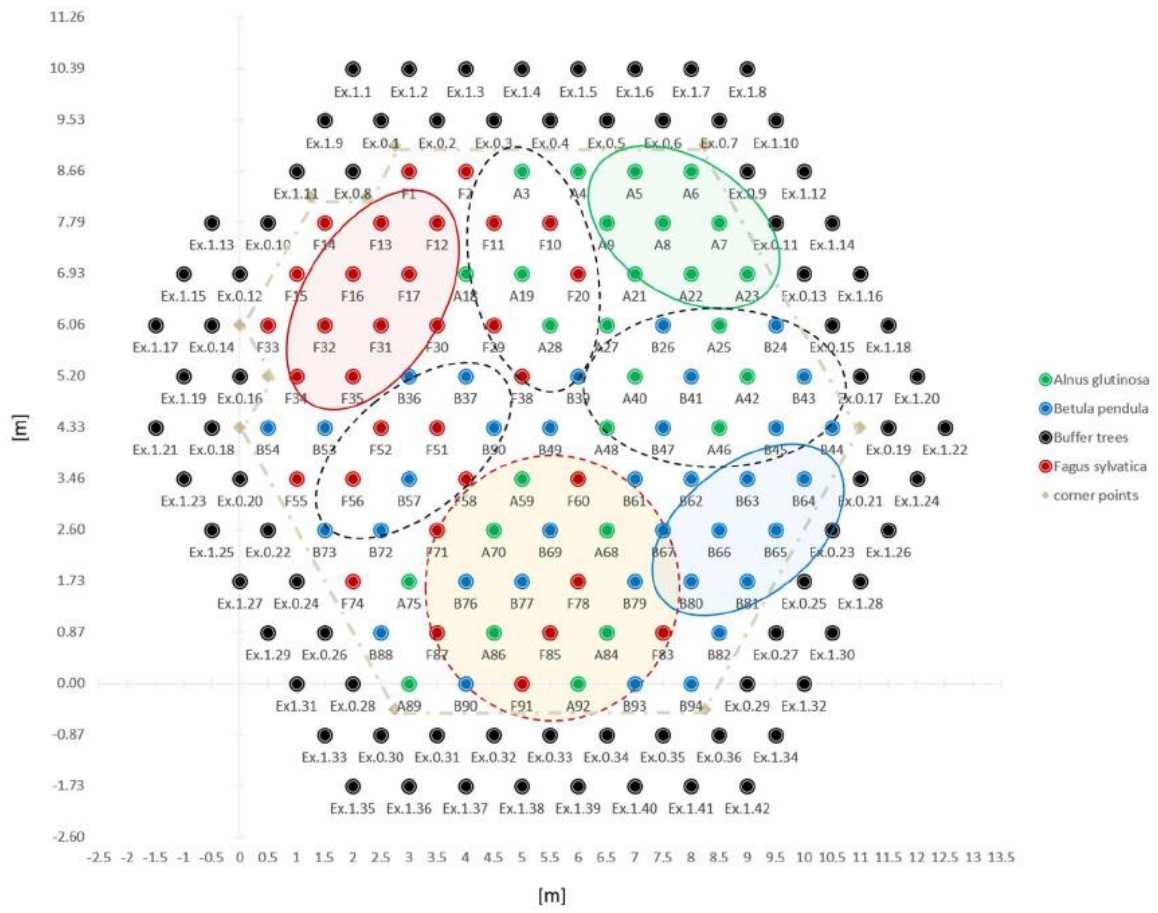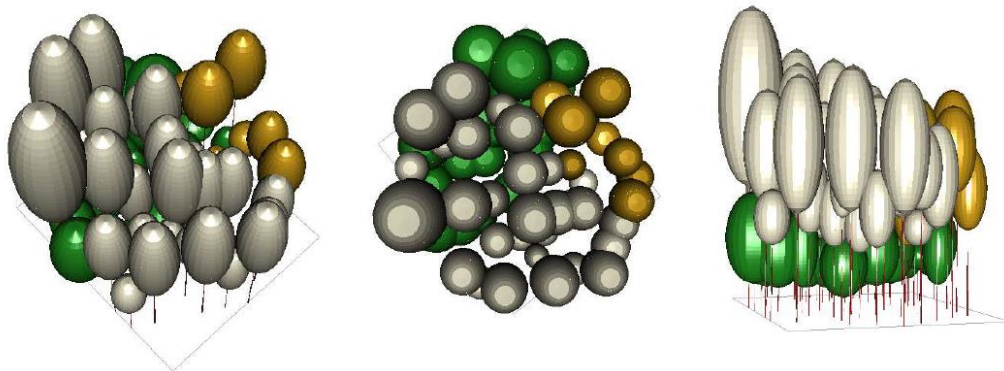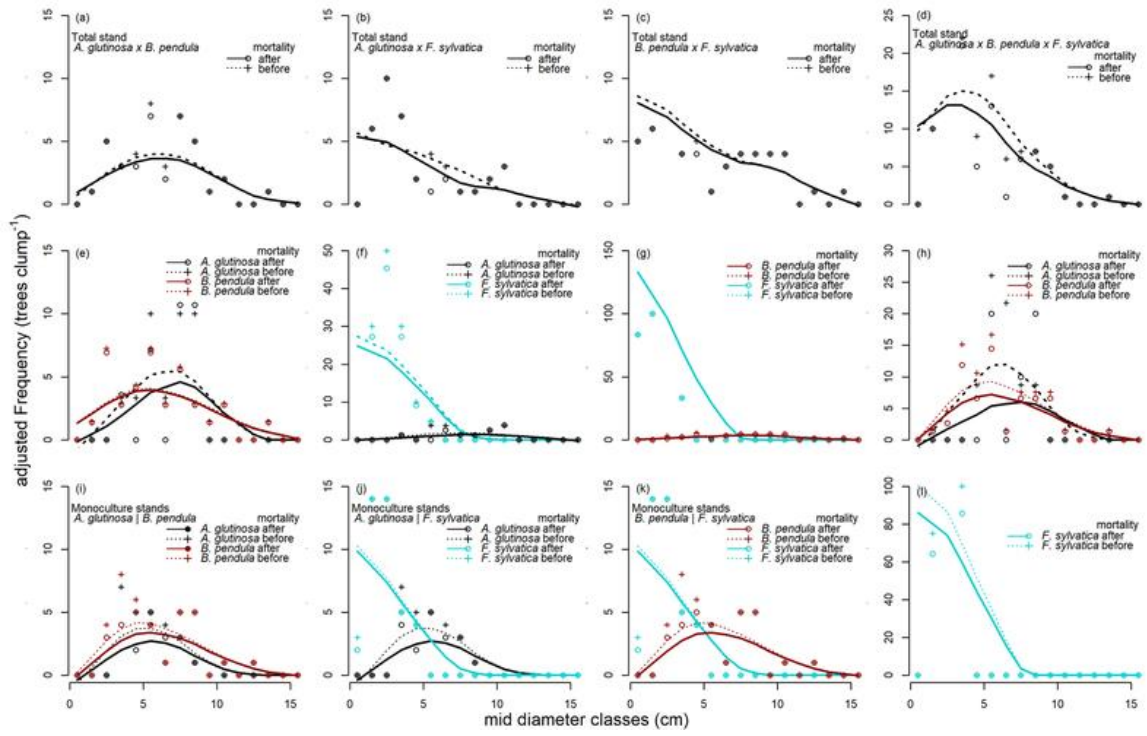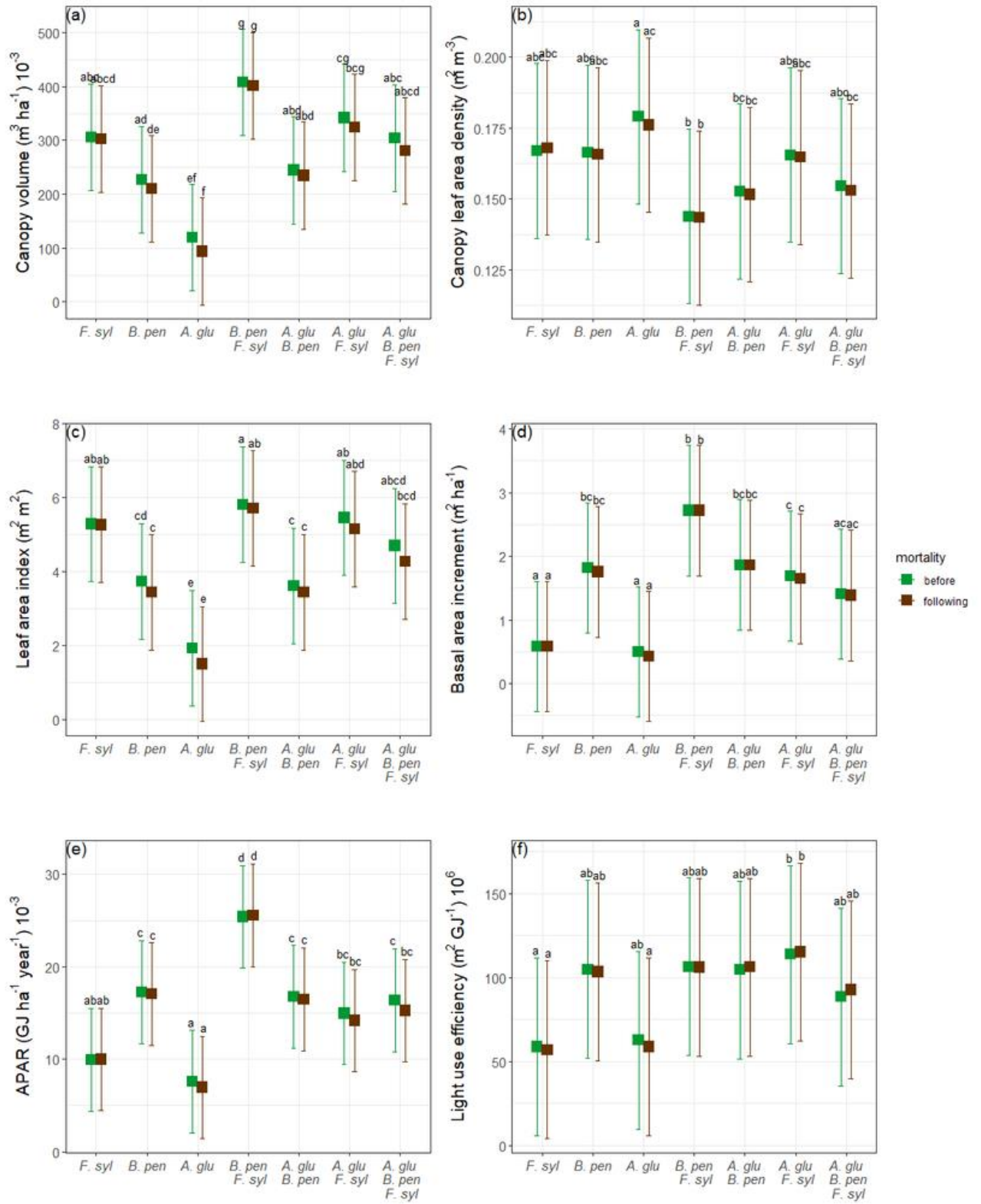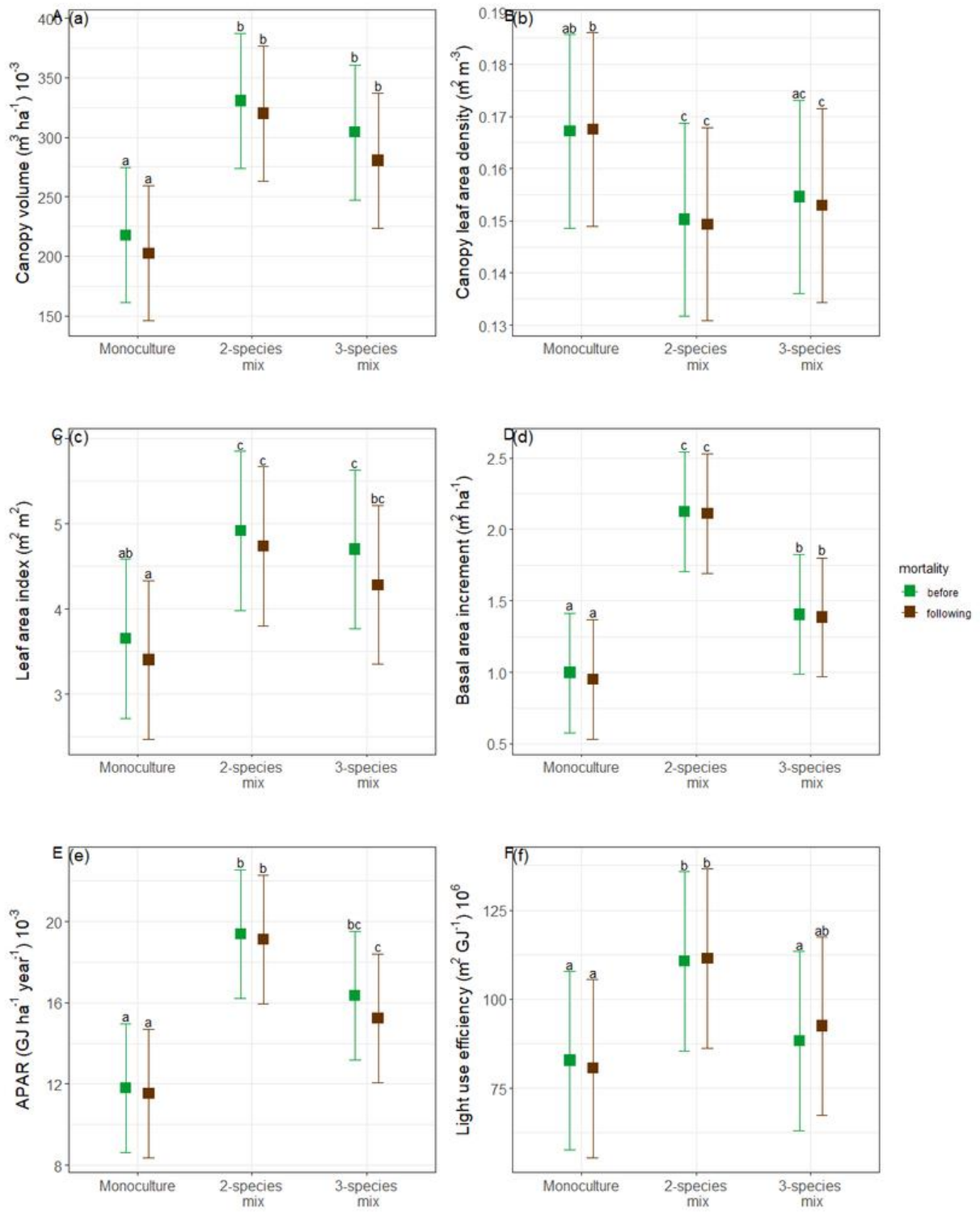
764

765

766

Figure 1

Figure 2

Figure 3

Figure 4

Figure 5